The apelin-apelin receptor signaling pathway in fibroblasts is involved in tumor growth via p53 expression of cancer cells

HIROTSUGU SAIKI[1*], YOSHITO HAYASHI[1], SHUNSUKE YOSHII[1*], EIJI KIMURA[1], KENTARO NAKAGAWA[1], MINORU KATO[1], RYOTARO UEMA[1], TAKANORI INOUE[1], AKIHIKO SAKATANI[2], TAKEO YOSHIHARA[1], YOSHIKI TSUJII[1], SHINICHIRO SHINZAKI[1], HIDEKI IIJIMA[1] and TETSUO TAKEHARA[1]

[1]Department of Gastroenterology and Hepatology, Osaka University Graduate School of Medicine, Yamadaoka, Suita, Osaka 565-0871; [2]Department of Gastroenterology and Hepatology, Osaka Police Hospital, Tennoji, Osaka 543-0035, Japan

Received July 27, 2023; Accepted October 18, 2023

DOI: 10.3892/ijo.2023.5587

Abstract. Cancer-associated fibroblasts (CAFs) are pivotal in tumor progression. TP53-deficiency in cancer cells is associated with robust stromal activation. The apelin-apelin receptor (APJ) system has been implicated in suppressing fibroblast-to-myofibroblast transition in non-neoplastic organ fibrosis. The present study aimed to elucidate the oncogenic role of the apelin-APJ system in tumor fibroblasts. APJ expression and the effect of APJ suppression in fibroblasts were investigated for p53 status in cancer cells using human cell lines (TP53-wild colon cancer, HCT116, and Caco-2; TP53-mutant colon cancer, SW480, and DLD-1; and colon fibroblasts, CCD-18Co), resected human tissue samples of colorectal cancers, and immune-deficient nude mouse xenograft models. The role of exosomes collected by ultracentrifugation were also analyzed as mediators of p53 expression in cancer cells and APJ expression in fibroblasts. APJ expression in fibroblasts co-cultured with p53-suppressed colon cancer cells ($HCT116^{sh\ p53}$ cells) was significantly lower than in control colon cancer cells ($HCT116^{sh\ control}$ cells). APJ-suppressed fibroblasts treated with an antagonist or small interfering RNA showed myofibroblast-like properties, including increased proliferation and migratory abilities, via accelerated phosphorylation of Sma- and Mad-related protein 2/3 (Smad2/3). In addition, xenografts of HCT116 cells with APJ-suppressed fibroblasts showed accelerated tumor growth. By contrast, apelin suppressed the upregulation of phosphorylated Smad2/3 in fibroblasts. MicroRNA 5703 enriched in exosomes derived from $HCT116^{sh\ p53}$ cells inhibited APJ expression, and inhibition of miR-5703 diminished APJ suppression in fibroblasts caused by cancer cells. APJ suppression from a specific microRNA in cancer cell-derived exosomes induced CAF-like properties in fibroblasts. Thus, the APJ system in fibroblasts in the tumor microenvironment may be a promising therapeutic target.

Introduction

Colorectal cancer has been one of the leading causes of cancer-related deaths worldwide, especially in patients with metastatic disease. The five-year survival rate of colorectal cancer patients is ~60%, but it decreases to 14% when distant metastases are present, regardless of the availability of several combination therapies as systemic treatments (1). Various genetic abnormalities such as wingless and int-1 (Wnt) signaling, tissue growth factor beta (TGFβ) signaling, or TP53 signaling have been known in the carcinogenesis of colorectal cancer (2,3). Although patients with a few specific biomarker-defined colorectal cancers, such as wild-type rat sarcoma viral oncogene homolog (RAS)/v-raf murine sarcoma viral oncogene homolog B (BRAF) and deoxyribonucleic acid mismatch repair-deficient/microsatellite instability-high, can already receive the benefits of additional chemotherapy to standard regimens (4-6), the development of a novel therapeutic target and chemotherapeutic agents for individualized treatment based on the respective genetic abnormalities is required to improve poor prognosis.

The tumor microenvironment consists of various cell types and fibroblasts in the tumor tissue, called cancer-associated fibroblasts (CAFs), which play pivotal role in tumor progression (7,8). CAFs and normal fibroblasts differ with respect to the expression of various markers, such as fibrotic markers,

Correspondence to: Professor Tetsuo Takehara, Department of Gastroenterology and Hepatology, Osaka University Graduate School of Medicine, 2-2, Yamadaoka, Suita, Osaka 565-0871, Japan
E-mail: takehara@gh.med.osaka-u.ac.jp

*Contributed equally

Abbreviations: α-SMA, alpha-smooth muscle actin; APJ, apelin receptor; ATCC, American Type Culture Collection; CAF, cancer-associated fibroblast; DMEM, Dulbecco's Modified Eagle Medium; EMEM, Eagle's Minimum Essential Medium; FBS, fetal bovine serum; PBS, phosphate-buffered saline; rhTGF-β1, recombinant human transforming growth factor-beta 1; shRNA, short hairpin RNA; TGFβ, transforming growth factor beta; TP53, tumor protein 53; WST, water-soluble tetrazolium

Key words: cancer-associated fibroblasts, colonic neoplasms, exosomes, microRNAs, tumor microenvironment

growth factors, chemokines and cytokines (9). CAFs with tumor-promoting effects were usually activated and exhibited myofibroblast-like properties such as the upregulation of alpha-smooth muscle actin (α-SMA) (9). TP53 is a significant tumor suppressor gene, and its somatic mutations are one of the most frequent alterations in ~50% of all human cancers, including colorectal cancer (10). The mutational inactivation of the TP53 gene in tumor cells has been reported to affect not only tumor cells but also the surrounding cells in the tumor microenvironment and to promote tumor-stromal activation and subsequent tumor growth (11,12). The secretion levels of various proteins, reactive oxygen species, or microRNAs (miRNAs) capsulized in exosomes have been reported as the mechanisms by which the alteration of TP53 status in tumor cells affects surrounding cells (11,12). These mechanisms may be involved in the transition of normal tissue fibroblasts to CAFs; however, the detailed mechanisms remain only partially understood.

The apelin-APJ system was first identified in 1993 as a G protein-coupled receptor, and apelin was isolated from bovine stomach extracts in 1998 as an endogenous ligand of APJ (13). Apelin and APJ are ubiquitously expressed throughout the organism and play several physiological roles (14,15). The apelin-APJ system in fibroblasts has been reported as a mechanism for suppressing the fibroblast-to-myofibroblast transition in non-neoplastic organ fibrosis, including myocardial fibrosis, pulmonary fibrosis, skin fibrosis and chronic kidney disease (16-19). It was posited by the authors that the APJ system could inhibit tumor-promoting CAFs, especially in acquiring myofibroblast characteristics. By contrast, the APJ system in tumor cells, not fibroblasts, including colorectal cancer cells, has also been reported to have a tumor-promoting effect (20-22) in contrast to the authors' hypothesis that the APJ system can play a role as a tumor suppressor via the inhibition of CAF activation in the tumor microenvironment. Although it is necessary to comprehensively view other types of cells in the tumor microenvironment, to the best of the authors' knowledge, no previous studies have described the significance of the APJ system in the tumor stroma. The present study aimed to elucidate the role of the APJ system in fibroblast modification in the tumor microenvironment of colorectal cancer, focusing on the p53 status of the cancer cells.

Materials and methods

Cell culture and treatment. The human colon cancer cell line HCT116 and Caco-2 exhibiting wild-type *TP53* expression, SW480 and DLD-1 of *TP53* mutant cells, and non-transformed human colon fibroblasts CCD-18Co were obtained from the American Type Culture Collection (ATCC). Cancer cells were cultured at 37˚C under 5% CO_2 in Dulbecco's Modified Eagle Medium (DMEM) (Sigma-Aldrich; Merck KGaA) supplemented with 10% fetal bovine serum (FBS) or Eagle's Minimum Essential Medium (EMEM) (ATCC) supplemented with 20% FBS, and fibroblasts were cultured at 37˚C under 5% CO_2 in EMEM with 10% FBS. To investigate the effect of apelin-13 (Cayman Chemical Company) on recombinant human TGF-β1 (rhTGF-β1)(FUJIFILM Wako Pure Chemical Corporation)-induced mRNA and protein expression in fibroblasts, the cells were pretreated with apelin-13 at the concentration of 10 to 1,000 nM for 60 min and then stimulated with rhTGF-β1 for 24-48 h. ML221 (Sigma-Aldrich; Merck KGaA), the APJ antagonist, was used to examine the effect of APJ suppression on fibroblasts at concentrations of 0.1 to 10 μM.

Exosome isolation. Cells were cultured in DMEM with 10% FBS in 15-cm dishes (Tissue Culture Dish VTC-D150, AS ONE CORPORATION) for 48 h, washed with phosphate-buffered saline (PBS), replaced with DMEM without FBS, and cultured for another 48 h, after which the culture supernatant was collected, and sequential centrifugation was performed. The culture supernatant was first centrifuged at 300 x g for 10 min at 4˚C, then at 2,000 x g for 10 min to precipitate the cells. The supernatant was then centrifuged at 10,000 x g for 30 min at 4˚C, and then ultra-centrifuged at 100,000 x g for 70 min at 4˚C to pellet the extracellular vesicles, which were then washed with a suspension in PBS. The final pellet was resuspended in 100 μl of PBS. The protein concentration was measured using a bicinchoninic acid (BCA) protein assay kit (Thermo Fisher Scientific, Inc.). Isolated exosomes were administered to fibroblasts culture supernatant at a concentration of 100 μg/ml. The morphology of the exosomes was captured using a transmission electron microscope (H-7600; Hitachi High-Technologies Corporation) after preparation as described here. A total of ~5 μl of sample was placed on Parafilm. Then, a carbon-coated 400 mesh copper grid was positioned on the top of the drop for 10 sec and washed by a droplet of distilled water. The grid was contrasted by adding a drop of 2% uranyl acetate on Parafilm and incubating the grid on the top of the drop for 10 sec. Excess liquid was removed by gently using an absorbent paper. After dying, the samples were used for observation. Furthermore, the expression of CD9, CD63 and ALIX, which are exosome markers, was confirmed by western blotting.

Co-culture experiment. Non-contact co-cultures were performed using Transwell inserts with 0.4-μm pores (Corning, Inc.). Fibroblasts or cancer cells were seeded on a six-well ($2x10^5$ cells per well) or 12-well ($3x10^4$ cells per well) plate (Corning, Inc.) in EMEM or DMEM with 10% FBS, and cancer cells or fibroblasts were seeded on a Transwell insert in the same conditions. After 24-48 h incubation, serum-free EMEM was used as the co-culture medium, and each culture was incubated for 48 h.

RNA interference. CCD-18Co cells were transfected for 48-72 h at 37˚C with small interfering (si)RNAs against APJ [Thermo Fisher Scientific, Inc.; #1; cat. no. s223458, 5'-CAG AUGCACGAGAAAUCCATT-3' (sense) and 5'-UGGAUU UCUCGUGCAUCUGTT-3' (antisense), #2; s1186, 5'-UGU GGGCUACCUACACGUAtt-3' (sense) and 5'-UACGUG UAGGUAGCCCACAgg-3' (antisense)], negative control siRNA (Thermo Fisher Scientific, Inc.; cat. no. 4390843), microRNA (miR)-5703 mimic (Thermo Fisher Scientific, Inc.; cat. no. 4464066), miR-5703 inhibitor (Thermo Fisher Scientific, Inc. cat. no. 4464084), miRNA mimic negative control (Thermo Fisher Scientific, Inc. cat. no. 4464058) and miRNA inhibitor negative control (Thermo Fisher Scientific, Inc. cat. no. 4464076) and SW480 cells were transfected with

RAB27A siRNA [Thermo Fisher Scientific, Inc.; cat. no. s532296; 5'-CCAGUGUACUUUACCAAUAtt-3' (sense) and 5'-UAUUGGUAAAGUACACUGGtc-3' (antisense)] at a final concentration of 10 nM using the Lipofectamine® RNAiMAX Reagent (Thermo Fisher Scientific, Inc.) according to the manufacturer's transfection protocol in six-well or 12-well plates (Corning, Inc.). In addition, as previously described (11), lentiviral GFP-IRES-short hairpin (sh)RNA vectors against TP53 (cat. nos. RHS4430-101161166; 101162286; 101168779; 99365289) were obtained from Thermo Fisher Scientific, Inc., and HCT116$^{sh\ control}$ and HCT116$^{sh\ p53}$ cells were generated. Cells with stable shRNA expression were cultured with 2 μg/ml puromycin (InvivoGen) after colony selection.

RNA/miRNA extraction and reverse transcription-quantitative (RT-q) PCR analysis. Total RNA or miRNAs were extracted and reverse transcribed as previously described (12). RNA was extracted from cells or nanovesicles using an RNeasy Mini Kit (cat. no. 74106; Qiagen GmbH) for mRNA and a miRNeasy Mini Kit (cat. no. 217084; Qiagen GmbH) for miRNAs according to the manufacturer's instructions. qPCR was performed using THUNDERBIRD qPCR Master Mix (Toyobo Life Science) on the QuantStudio 6 Flex (Applied Biosystems; Thermo Fisher Scientific, Inc.). The thermocycling conditions of the qPCR reaction were: 20 sec of initial denaturation at 95˚C; followed by 40-60 cycles of 1 sec at 95˚C for denaturation, and 20 sec at 60˚C for annealing and extension. The mRNA expression was quantified using TaqMan gene expression assays (Applied Biosystems; Thermo Fisher Scientific, Inc.), and data were normalized to beta-2-microglobulin (B2M) expression levels. The miRNAs were reverse transcribed using miRNA-specific primers (Applied Biosystems; Thermo Fisher Scientific, Inc.), and miRNA expression was quantified using TaqMan gene expression assays. Data were normalized to the expression of spike-in syn-cel-miR-39 (Qiagen). The $2^{-\Delta\Delta Cq}$ method was used to analyze the relative gene expression as previously described (23). The used primers are listed in Table SI.

Western blotting. Protein extracts were prepared as previously described (11). Cells were lysed with radio-immunoprecipitation assay (RIPA) buffer containing protease inhibitor and phosphatase inhibitor cocktail (Nacalai Tesque, Inc.), and the proteins were collected on ice. The protein concentration was measured by the BCA protein assay kit. Equal amounts of protein (10 μg) were applied to each lane of 8% sodium dodecyl sulfate-polyacrylamide gel electrophoresis (SDS-PAGE) gels and run. The proteins were then transferred onto polyvinylidene difluoride (PVDF) membranes and blocked with 4% milk in 0.1% Tris-buffered saline with Tween-20 (TBST) at room temperature for 1 h. Then, each membrane was subjected to overnight incubation at 4˚C with the appropriate primary antibodies for β-actin (1:1,000; cat. no. 4970; Cell Signaling Technology, Inc.), TP53 (1:200; cat. no. sc-126; Santa Cruz Biotechnology, Inc.), APJ (1:1,000; cat. no. ab84296; Abcam or 1 μg/ml, cat. no. 702069; Thermo Fisher Scientific, Inc.), α-SMA (1:1,000; cat. no. ab5694; Abcam), phosphorylated Smad2/3 (1:1,000; cat. no. 8828; Cell Signaling Technology, Inc.) and Smad2/3 (1:1,000; cat. no. 3102, Cell Signaling Technology, Inc.). After incubation, the membranes were incubated with horseradish peroxidase (HRP)-conjugated secondary antibody (1:3,000; cat. no. NA934-1ML; Cytiva) at room temperature for 60 min. Finally, the membranes were reacted with detection reagents (Super Signal West Pico PLUS Chemiluminescent Substrate; Thermo Fisher Scientific, Inc.) and exposed for an appropriate time to visualize the protein bands using the ChemiDoc MP (Bio-Rad Laboratories, Inc.). Primary antibodies used for western blotting are listed in Table SII.

Cell proliferation assay. Cell proliferation and viability were analyzed in 12-well plates ($3x10^4$ cells per well). Water-soluble tetrazolium (WST) assays were performed using an SF cell counting reagent (Nacalai Tesque, Inc.). A total of 100 μl reagent was added to 1,000 μl culture medium per well. After 30 min of incubation at 37˚C, the absorbance was measured at 450 nm with 600 nm used as a reference with a microplate reader (Thermo Fisher Scientific, Inc.).

Cell wound healing assay. Wound healing assay was performed to assess the migratory ability of fibroblasts. Cells seeded on a six-well plate ($2x10^5$ cells per well) were incubated for 24 h; thereafter, the medium was changed to serum-free, ML221 was applied, and cells were scratched using the tip of the 200-μl sterile pipette tube. In the same manner, cells were seeded on a six-well plate ($2x10^5$ cells per well), were transfected with siRNA against APJ, and incubated for 24 h. Next, the medium was changed and incubated for another 24 h, after which cells were scratched the same as aforementioned. The wound reduction rates were calculated by measuring the area of the wound after 0 and 24 h in 3 microscopic fields (magnification, x200; BZ-X700 all-in-one fluorescence microscope; Keyence Corporation), which were randomly selected.

Immunofluorescence staining. Fibroblasts were seeded on a 35-mm dish (Matsunami Glass Ind., Ltd.) ($2x10^5$ cells per dish) and were transfected with siRNA against APJ 72 h before the experiment or were treated with ML221 (10 μM) 24 h prior to the experiment. Cells were fixed with 100% methanol at room temperature for 15 min. After cells were blocked with 1% bovine serum albumin (Nacalai Tesque, Inc.), the primary antibody reaction against anti-α-SMA (1:400; cat. no. ab5694; Abcam) was performed at room temperature for 1 h. Following a secondary antibody reaction using Alexa Fluor Plus 488 (1:1,000; cat. no. 4412; Cell Signaling Technology, Inc.) at room temperature for 1 h, nuclear staining was performed using Hoechst (1:200; cat. no. 346-07951; Dojindo Laboratories, Inc.) at room temperature for 10 min. The images were analyzed using a fluorescence microscope (BZ-X700 all-in-one fluorescence microscope; Keyence Corporation). The antibody used for fluorescent immunostaining is listed in Table SII.

Immunohistochemistry. Immunohistochemical staining for p53 and APJ in colorectal cancers with submucosal invasion was performed using endoscopically resected specimens at the Osaka University Hospital between April 2015 and August 2020. The paraffin-embedded tumor tissues were cut into 4-μm sections. The sections were dewaxed with xylene, dehydrated with descending ethanol series, activated with antigen retrieval citrate buffer, and incubated with 3% H_2O_2 at room temperature for 10 min. The slides were blocked with serum-free

phosphate buffer including casein at room temperature for 20 min and incubated with the primary antibodies at 4˚C overnight. The primary antibodies were as follows: anti-P53 (1:100; cat. no. sc-126; Santa Cruz Biotechnology, Inc.) or anti-APJ (1:100; cat. no. ABD43; Sigma-Aldrich; Merck KGaA). The sections were incubated with HRP-conjugated secondary antibody (no dilution; cat. no. K5007; Agilent Technologies, Inc.) at room temperature for 20 min and counterstained with hematoxylin at room temperature for 15 sec. The slides were captured using a light microscope (VS200; Olympus Corporation). The expression of p53 in cancer cells, of APJ in fibroblasts from the tumor stroma, and of α-SMA in the stroma with HALO software were quantified (Indica Labs, Inc.). p53 expression was assessed using a previously described scoring method (24). The p53 expression levels were evaluated according to the positive rate of p53 staining in tumor cells, and p53 positivity was defined as more than 10% of p53 positive staining. APJ expression levels were assessed by calculating the H-score using the software. The area of α-SMA staining in the stroma was calculated by the aforementioned software. The antibodies used for immunohistochemistry in each case are listed in Table SII.

Xenograft model. HCT116 cells ($2x10^5$) were suspended in 200 μl of PBS and co-inoculated with negative control-transfected CCD-18Co cells ($2x10^5$) and CCD-18Co cells with suppressed APJ expression ($2x10^5$) subcutaneously into the left and right flank of 5-6-week-old male BALB/c nude mice (Charles River, Yokohama, Japan), respectively (each group n=10). A total of 20 mice were used. All mice were housed in a specific pathogen free condition at a constant temperature of 23±1.5˚C with 45±15% humidity under a 12/12-h light/dark cycle and were fed with MFG (Oriental Yeast Co., Ltd.) with free access to water. In addition, gene suppression using siRNA in the xenograft experiments was performed as previously described. At the time of subcutaneous implantation, the mice were anesthetized with medetomidine hydrochloride (0.75 mg/kg), midazolam (4 mg/kg) and butorphanol tartrate (5 mg/kg). Tumor volume was measured three times a week and calculated using the formula: [tumor length x (tumor width)^2]/2. Humane endpoints were set at a tumor volume of 2,000 mm^3 and irreversible wasting. The duration of the experiment was 21 days. The last measurement of the tumor volume was obtained on the 21st day, followed by euthanasia by CO_2 administration with a fill rate of 30-70% of the chamber volume per min and death was verified by checking for the heartbeat and breath cessation. All mice used were euthanized.

Bioinformatics analysis. The National Center for Biotechnology Information Gene Expression Omnibus (NCBI GEO) database and miR-DB database (http://mirdb.org) were used in the present study. To analyze APJ expression in colon fibroblasts, NCBI GEO database (accession no. GSE46824; https://www.ncbi.nlm.nih.gov/geo/query/acc.cgi?acc=GSE46824) was used. NCBI GEO database (accession no. GSE120012; https://www.ncbi.nlm.nih.gov/geo/query/acc.cgi?acc=GSE120012) and miR-DB database were used to analyze miR-5703.

Statistical analysis. Data were expressed as the mean ± standard deviation. The two-tailed, paired or unpaired Student's t-test was used to compare two groups. A one-way analysis of variance (ANOVA) with Tukey's post hoc test was performed to analyze the differences among multiple groups. $P<0.05$ was considered to indicate a statistically significant difference. The statistical analyses were performed using the JMP® Pro15 software (SAS Institute Inc.).

Study approval. The present study was approved (approval no. 20061) by the Ethics Committee of Osaka University Graduate School of Medicine (Osaka, Japan) for using resected human samples, and written informed consent was obtained from all patients who provided resected specimens. The study design was per the principles of the Declaration of Helsinki (October 2013). The animal experimental procedures were performed per the Osaka University guidelines for animal experiments and were approved (approval no. 30-015-077) by the Animal Care and Use Committee of Osaka University Graduate School of Medicine (Osaka, Japan).

Results

Colorectal cancer cells with p53-inactivation suppress APJ expression in fibroblasts. First, non-contact cell co-culture experiments were conducted using a Transwell insert for fibroblasts (CCD-18Co). To investigate the involvement of p53 inactivation in cancer cells with APJ expression in fibroblasts, p53-suppressed colorectal cancer cells, HCT116$^{sh\ p53}$ cells, were established. Successful inhibition of TP53 expression in HCT116$^{sh\ p53}$ cells was confirmed by RT-qPCR and western blotting (Figs. 1A and S1A). The expression level of APJ in CCD-18Co cells was decreased along with increased expression of α-SMA when co-cultured with HCT116$^{sh\ p53}$ cells compared with co-cultured with HCT116$^{sh\ control}$ cells or CCD-18Co cells alone in western blotting (Figs. 1B and S1B). The mRNA levels of TGFβ1 and VEGF-A expression in fibroblasts significantly increased when co-cultured with HCT116$^{sh\ p53}$ cells (Fig. 1C). In addition, the expression levels of APJ were decreased and α-SMA were increased in fibroblasts when co-cultured with TP53-mutant colon cancer cells such as SW480 or DLD-1 cells, in contrast to TP53-wild colon cancer cells such as HCT116 or Caco-2 (Figs. 1D and S1C and D). The mRNA expression levels of TGFβ1 and VEGF-A were significantly increased when co-cultured with SW480 and DLD-1 cells as observed in HCT116$^{sh\ p53}$ cells, which were also significantly increased than those co-cultured with HCT116 and Caco-2 cells (Fig. 1E).

Next, APJ expression was examined in fibroblasts from human colorectal cancer tissues. APJ expression levels in cancer stromal fibroblasts were evaluated based on the p53 status of colorectal cancer cells. Immunohistochemical staining was performed for p53, APJ and α-SMA in endoscopically resected cancers with submucosal invasion. The patient and lesion characteristics are summarized in Table SIII. The APJ staining score in cancer stromal fibroblasts was significantly lower in p53-positive (suggesting p53 mutation) colorectal cancers than in p53-negative (suggesting wild-type p53) colorectal cancers. The APJ staining score was assessed separately in the left colon (descending colon, sigmoid colon, rectum) and right colon (cecum, ascending colon, transverse

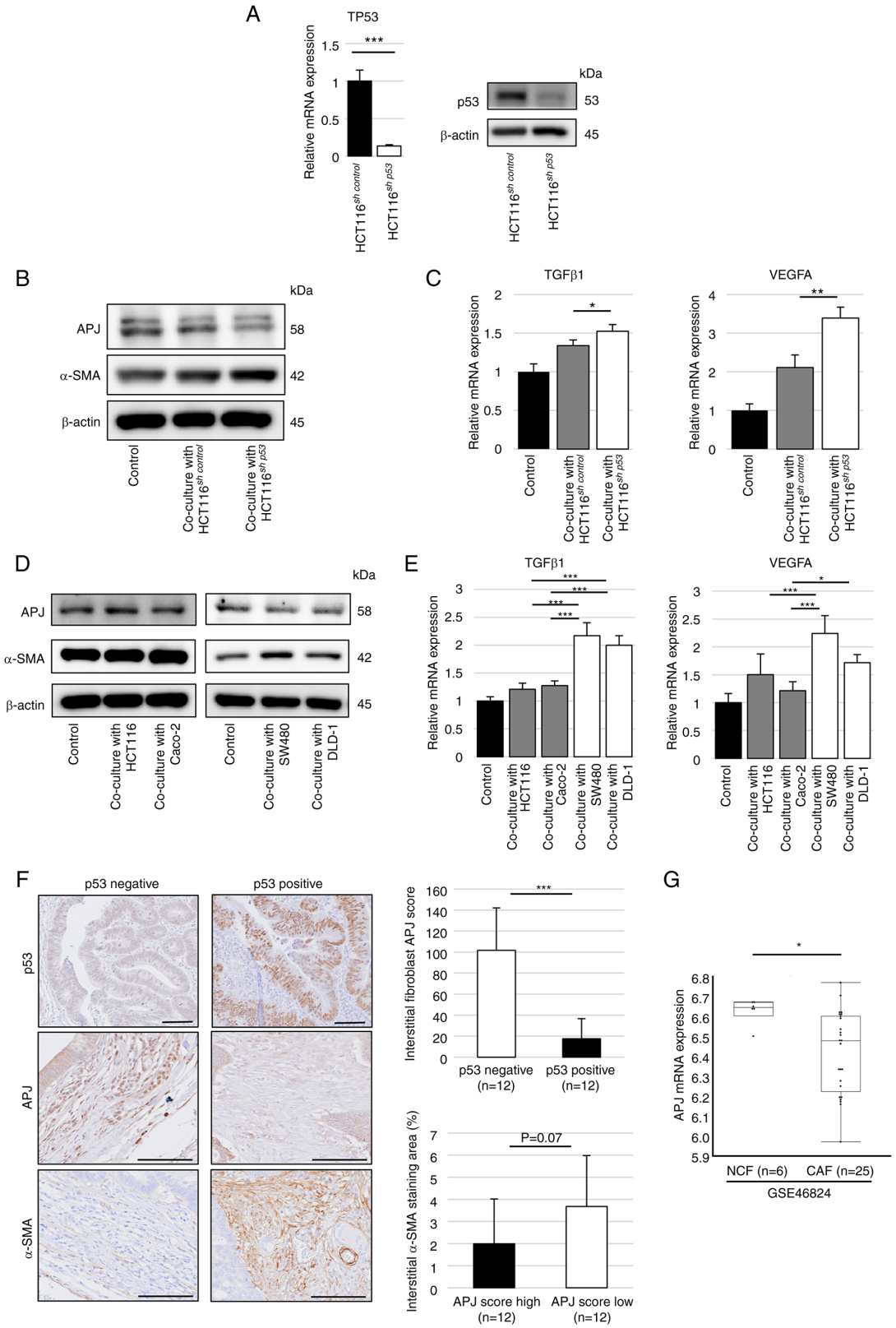

Figure 1. Colon cancer cells with deficient or mutated TP53 function suppress APJ expression in CCD-18Co cells. (A) RT-qPCR was performed to assess TP53 mRNA expression in HCT116$^{sh\ control}$ or HCT116$^{sh\ p53}$ cells (left). Western blotting was performed for TP53 (right). (B) Western blot analysis of APJ and α-SMA in CCD-18Co cells co-cultured with HCT116$^{sh\ control}$ or HCT116$^{sh\ p53}$ cells. The immunoblots were performed three times. (C) RT-qPCR was performed to assess TGFβ1 and VEGFA mRNA expression in CCD-18Co cells co-cultured with HCT116$^{sh\ control}$ or HCT116$^{sh\ p53}$ cells. (D) Western blotting was performed for APJ and α-SMA expression in CCD-18Co cells co-cultured with HCT116 or Caco-2 cells (left) and SW480 or DLD-1 cells (right). The immunoblots were performed three times. (E) Relative mRNA expression levels of TGFβ1 and VEGFA in CCD-18Co cells co-cultured with or without HCT116, Caco-2, SW480, or DLD-1 cells. (F) Immunohistochemical staining of APJ in colon cancer tissues. Representative images of positive and negative p53 expression, high and low APJ scores, and α-SMA staining. Scale bar, 100 μm. (G) APJ expression of fibroblasts in non-tumor and colon cancer tissues from (Gene Expression Omnibus) database. Data are presented as the mean ± SD. A one-way ANOVA with Tukey's post hoc test was performed to analyze the differences among multiple groups. *P<0.05, **P<0.01 and ***P<0.001. APJ, apelin receptor; RT-qPCR, reverse transcription-quantitative PCR; shRNA, short hairpin RNA; α-SMA, alpha-smooth muscle actin; NCF, normal colonic fibroblasts; CAF, cancer-associated fibroblasts.

colon), but there were no significant differences (Fig. S9). The relationship between clinicopathological characteristics and p53 status of endoscopic-resected cases is listed in Table SIV. Next, the included cases were divided into two groups according to their median APJ staining score (high or low). The area of α-SMA staining in each of these groups was then estimated, which showed a trend towards being larger in the low score group (Fig. 1F). mRNA expression datasets of fibroblasts extracted from fresh surgical specimens of colorectal carcinoma (CAF group) and normal colonic mucosa (normal colonic fibroblasts, NCF group) were obtained using NCBI GEO database (accession no. GSE46824). The datasets revealed that APJ expression was significantly lower in the CAF group than in the NCF group (Fig. 1G). These results indicated that *TP53*-inactivated colorectal cancer cells inhibit APJ expression in fibroblasts and induce fibroblast modification with myofibroblast-like properties.

APJ inhibition in fibroblasts by APJ antagonist induces the modification into myofibroblasts-like properties. Experiments using ML221 in CCD-18Co cells were performed to investigate the significance of APJ inhibition in colon fibroblast modification. The relative mRNA expression levels of TGFβ1, VEGF-A and ACTA2 were significantly increased in CCD-18Co cells with ML221 compared with control, and the western blotting analysis revealed increased α-SMA protein levels with ML221 (Figs. 2A and S2). α-SMA expression was next visualized using fluorescence immunostaining, and the expression of α-SMA was revealed to be significantly stronger in CCD-18Co cells with ML221 than in the control (Fig. 2B). A wound healing assay of CCD-18Co cells to examine the migration ability. The wound healing of CCD-18Co cells treated with ML221 was significantly faster than that of the control cells (Fig. 2C). Cell proliferation was also examined using a WST assay. Adding ML221 significantly increased the proliferation of CCD-18Co cells compared with the control in ML221 dose-dependent manner (Fig. 2D). Furthermore, the proliferation of colon cancer cells, which was increased by co-culture with CCD-18Co cells, was significantly increased by adding ML221 to CCD-18Co cells (Fig. 2E).

APJ suppression in fibroblasts induces the modification into myofibroblasts-like properties. Next, APJ expression was suppressed in fibroblasts using APJ siRNA. The APJ mRNA and protein expression levels were successfully suppressed by siRNA with elevated α-SMA expression levels. The relative mRNA expression levels of TGFβ1, VEGF-A and ACTA2 were significantly increased with siRNA for APJ compared with the control (Figs. 3A and S3). α-SMA expression was also visualized using fluorescence immunostaining, and α-SMA was more strongly expressed in APJ-suppressed CCD-18Co cells than in the control (Fig. 3B). Wound healing assay revealed that the migration ability of APJ-suppressed CCD-18Co cells was significantly increased compared with that of the control (Fig. 3C). The WST assay revealed that the viability of APJ-suppressed CCD-18Co cells was significantly higher than that of the control (Fig. 3D).

Next, regarding fibroblast-mediated tumor growth, the importance of APJ expression of fibroblasts was investigated using TP53-wild cancer cells in xenograft experiments. Tumor volumes of co-implanted HCT116 and CCD-18Co cells were significantly higher than those of HCT116 cells alone, and APJ suppression in CCD-18Co cells promoted faster tumor growth than the control (Fig. 3E). These results suggest that suppression of APJ in fibroblasts induces modification of myofibroblast-like properties and accelerates tumor growth.

TGFβ-Smad pathway is activated in APJ-suppressed colon fibroblasts. It has been reported that TGFβ1 induces α-SMA production via phosphorylated Sma- and Mad-related protein 2/3 (Smad2/3); the addition of apelin inhibits the induction of phosphorylated Smad2/3 by TGFβ1 (18,19). Next, the TGFβ-Smad pathway was evaluated in fibroblasts as a mechanism by which the apelin-APJ system can suppress the modification of fibroblasts into myofibroblasts-like properties. The mRNA expression levels of TGFβ1, VEGF-A and ACTA2 in CCD-18Co cells were increased by rhTGF-β1 stimulation. These increased expression levels were diminished significantly by the addition of recombinant human apelin-13 (Fig. 4A), suggesting the apelin-APJ system could suppress the TGFβ-induced fibroblasts modification. Western blot analysis revealed that phosphorylated Smad2/3 and α-SMA protein levels in CCD-18Co cells, which were increased by rhTGF-β1 stimulation, were decreased by adding recombinant human apelin-13 (Figs. 4B and S4). Increased expression of phosphorylated Smad2/3 was also found in CCD-18Co cells whose APJ expression was suppressed by ML221, siRNA or co-cultured cancer cells (Figs. 4C and S5A-D). These results suggested that the apelin-APJ system inhibits the TGFβ-Smad pathway in fibroblasts.

Cancer cell-derived exosomes suppress APJ expression in fibroblasts. Cancer cell-derived exosomes and encapsulated miRNAs are crucial communication tools in the tumor microenvironment (12). Moreover, alterations in TP53 expression in donor cancer cells have been reported to modify their exosomal miRNA profiles and affect the expression of several genes in the surrounding recipient cells (25,26). Cancer cell-derived exosomes were used to explore the mechanisms underlying APJ suppression in colon fibroblasts. Exosomes were collected from HCT116$^{sh\ control}$ and HCT116$^{sh\ p53}$ cells culture supernatants by the ultracentrifugation method and the expression of CD9, CD63 and ALIX, which are exosome markers, was confirmed by western blotting. The size and morphology of isolated exosomes were determined by transmission electron microscopy (Figs. 5A and S6). Furthermore, no significant differences were observed in the protein levels of the pellets isolated from HCT116$^{sh\ control}$ and HCT116$^{sh\ p53}$ cell culture supernatants (Fig. 5B). CCD-18Co cells were stimulated with HCT116$^{sh\ control}$- or HCT116$^{sh\ p53}$-derived exosomes to confirm the effects of the exosomes. Western blotting demonstrated that APJ expression was decreased in CCD-18Co cells transfected with HCT116$^{sh\ p53}$-derived exosomes (Figs. 5C and S7A). In addition, the relative expression levels of TGFβ1, VEGF-A, and ACTA2 in mRNA were significantly increased with HCT116$^{sh\ p53}$-derived exosomes (Fig. 5D).

Next, exosomes were collected from the culture supernatant of SW480 cells by ultracentrifugation. When the exosomes were added to CCD-18Co cells, the protein expression of APJ in CCD-18Co cells was decreased with SW480-derived

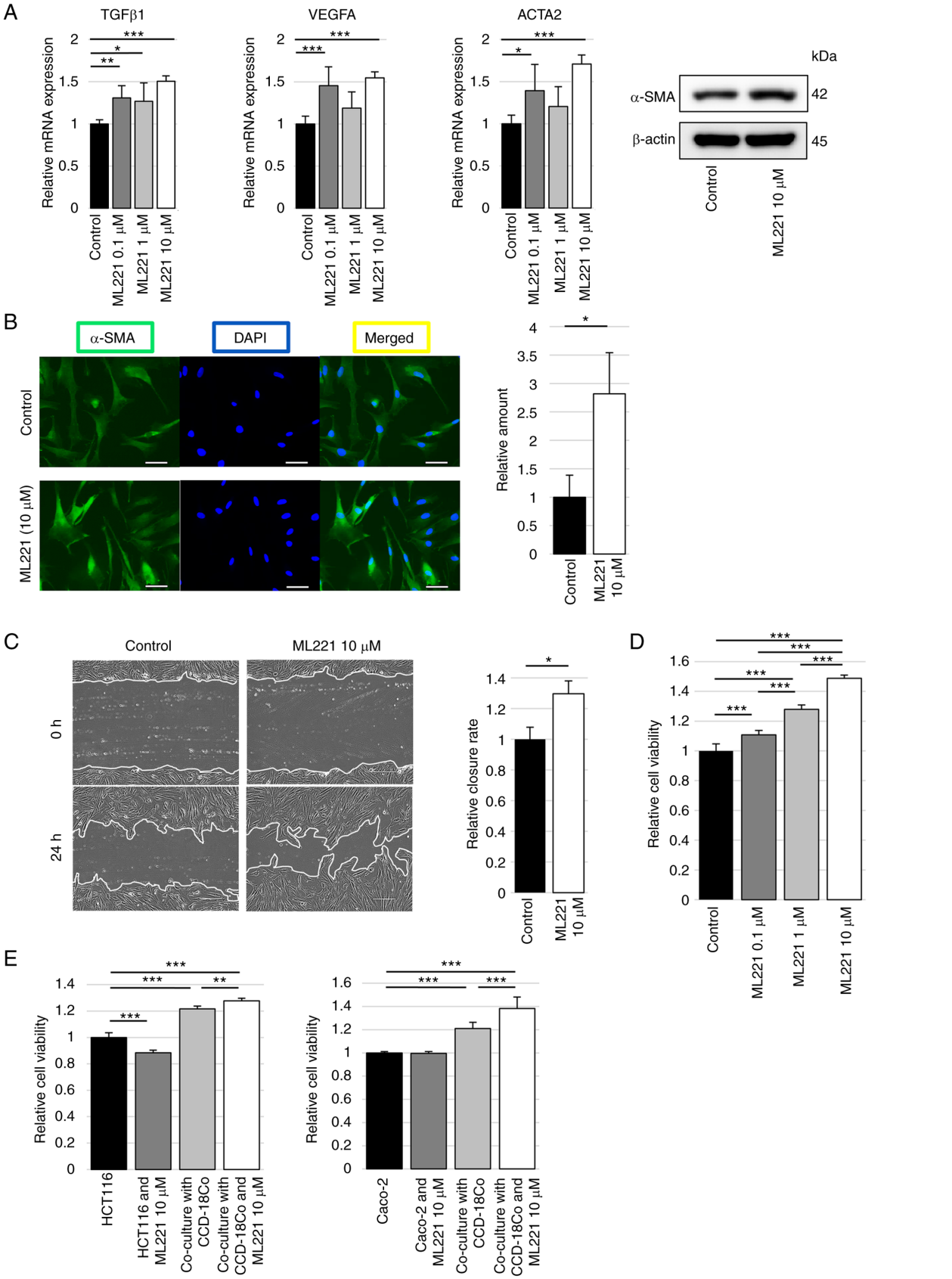

Figure 2. APJ suppression promotes the viability and migratory ability of CCD-18Co cells. (A) Reverse transcription-quantitative PCR was performed to evaluate TGFβ1, VEGFA and ACTA2 mRNA expression in CCD-18Co cells with or without ML221 in the concentration range of 0.1-10 μM (left). Western blot analysis of α-SMA in CCD-18Co cells with ML221 (10 μM) (right). The immunoblots were performed three times. (B) Immunofluorescence images of CCD-18Co cells with ML221 (10 μM) compared with control. Scale bar, 50 μm. (C) Cell wound healing assay of CCD-18Co cells with ML221 (10 μM) compared with control. Scale bar, 200 μm. (D) WST assay of CCD-18Co cells with ML221 in the concentration range of 0.1-10 μM compared with control. (E) WST assay of HCT116 and Caco-2 cells with or without CCD-18Co cells and ML221 (10 μM). Data are presented as the mean ± SD. A one-way ANOVA with Tukey's post hoc test was performed to analyze the differences among multiple groups. *P<0.05, **P<0.01 and ***P<0.001. α-SMA, alpha-smooth muscle actin.

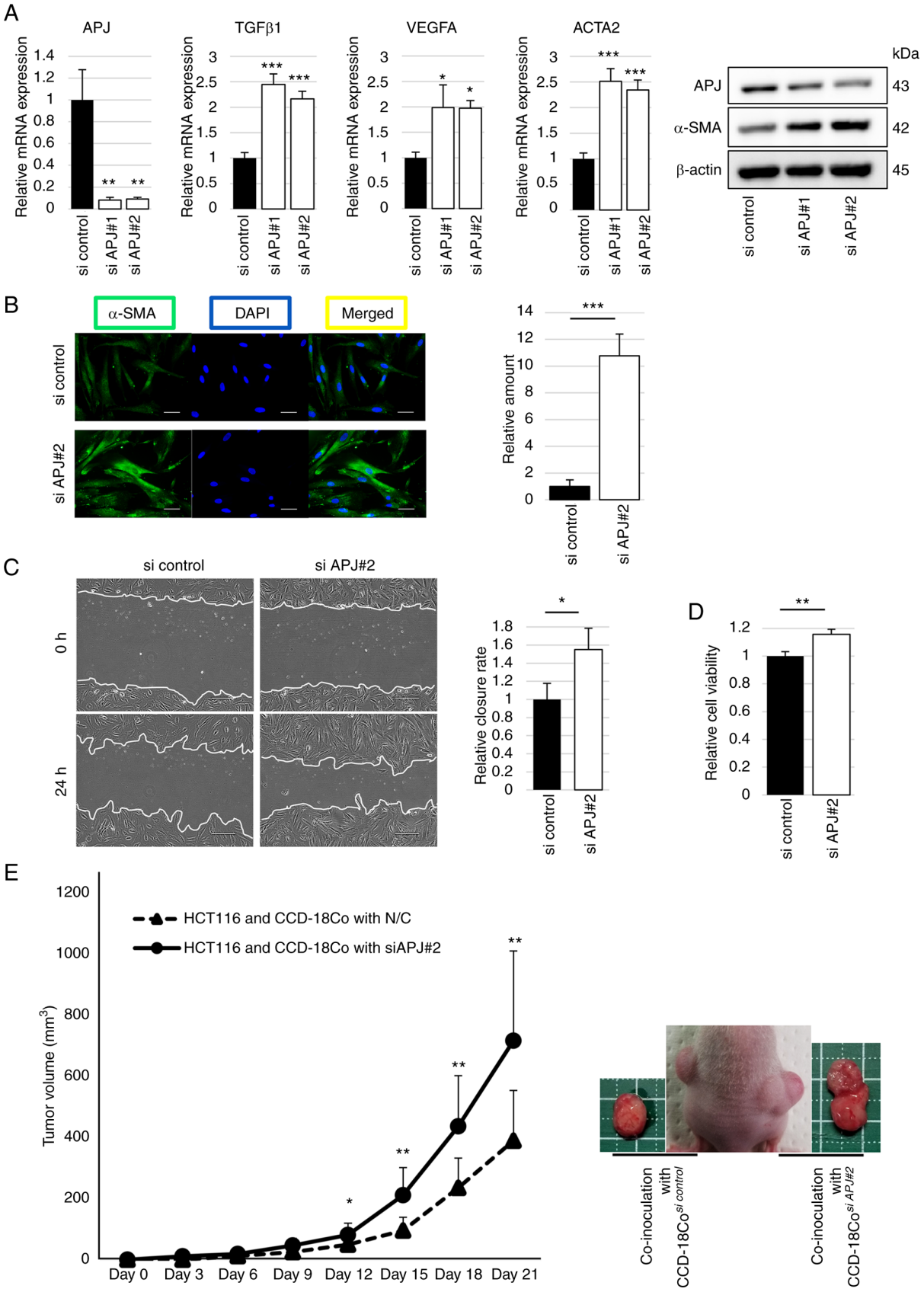

Figure 3. APJ suppression in CCD-18Co cells involves cancer cell proliferation and tumor growth. (A) Reverse transcription-quantitative PCR was performed to assess APJ, TGFβ1, VEGFA and ACTA2 mRNA expression in CCD-18Co cells with APJ siRNA compared with si control (left). Western blot analysis of APJ and α-SMA in CCD-18Co cells with APJ siRNA compared with si control (right). The immunoblots were performed three times. (B) Immunofluorescence images of CCD-18Co cells with APJ siRNA compared with si control. Scale bar, 50 μm. (C) Cell wound healing assay of CCD-18Co cells with APJ siRNA compared with si control. Scale bar, 200 μm. (D) WST assay of CCD-18Co cells with APJ siRNA compared with si control. (E) Tumor volume of HCT116 cells injected subcutaneously into BALB/c nude mice with CCD-18Co cells with APJ siRNA. Data are presented as the mean ± SD. A one-way ANOVA with Tukey's post hoc test was performed to analyze the differences among multiple groups. *P<0.05, **P<0.01 and ***P<0.001. siRNA, short interfering RNA; α-SMA, alpha-smooth muscle actin; APJ, apelin receptor.

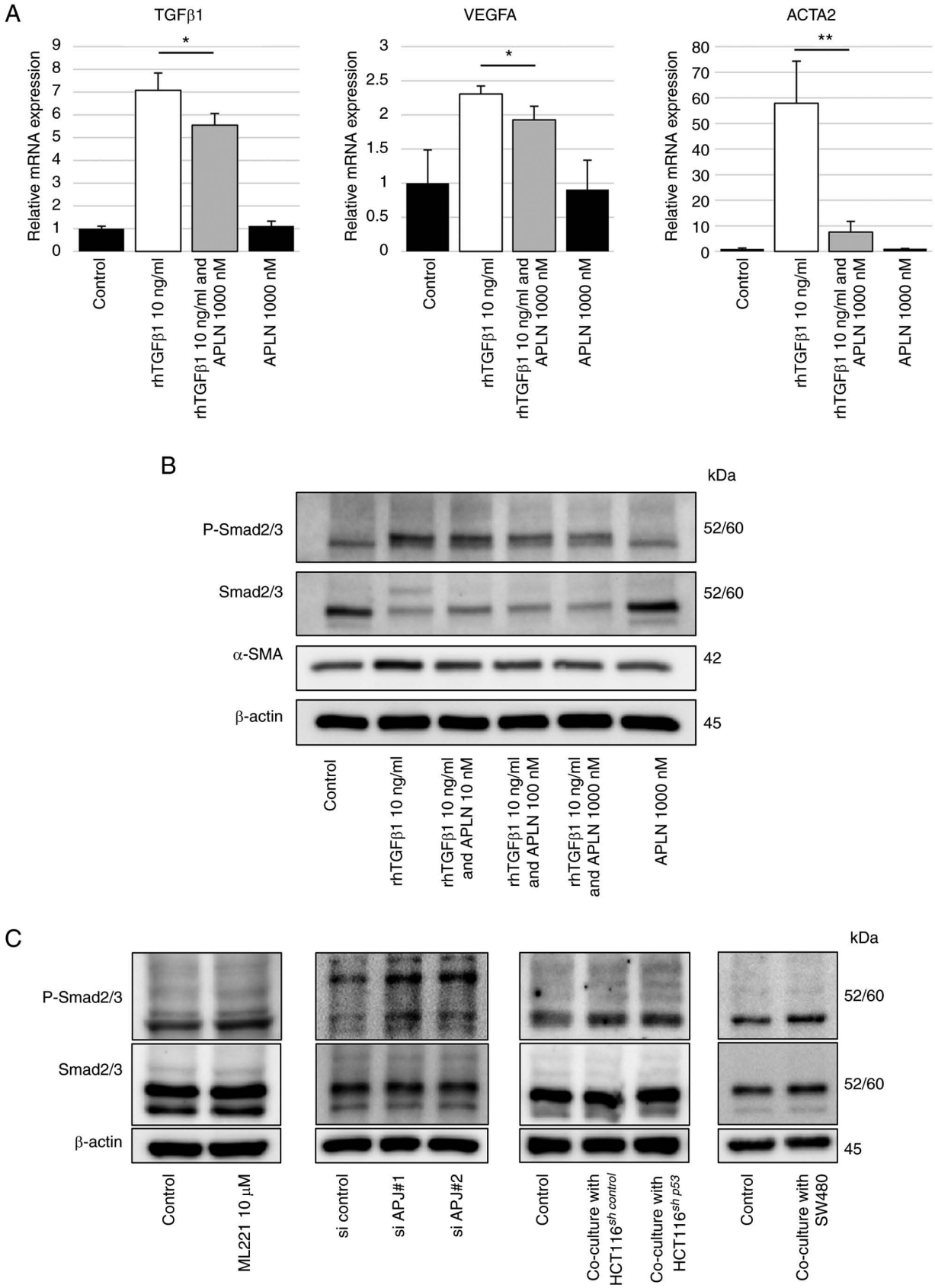

Figure 4. The APJ system inhibits TGFβ1-Smad signaling in CCD-18Co cells. (A) Reverse transcription-quantitative PCR was performed to assess TGFβ1, VEGFA and ACTA2 mRNA expression in CCD-18Co cells treated with or without apelin-13 (1,000 nM) and/or rhTGF-β1 (10 ng/ml). (B) Western blot analysis of phosphorylated Smad2/3, Smad2/3 and α-SMA in CCD-18Co cells with or without apelin-13 in the 10-1,000 nM range and/or rhTGF-β1 (10 ng/ml). (C) Western blotting was performed for phosphorylated Smad2/3 and Smad2/3 in CCD-18Co cells with ML221 (10 μM), with APJ siRNA, co-cultured with HCT116$^{sh\ control}$ or HCT116$^{sh\ p53}$ cells, and co-cultured with SW480 cells, compared with control, respectively. The immunoblots were performed three times. Data are presented as the mean ± SD. *P<0.05, and **P<0.01 vs. TGFβ1 group. APJ, apelin receptor; rhTGF-β1, recombinant human transforming growth factor beta 1; APLN, apelin-13; P-Smad2/3, phosphorylated Smad2/3; α-SMA, alpha-smooth muscle actin; siRNA, short interfering RNA; shRNA, short hairpin RNA.

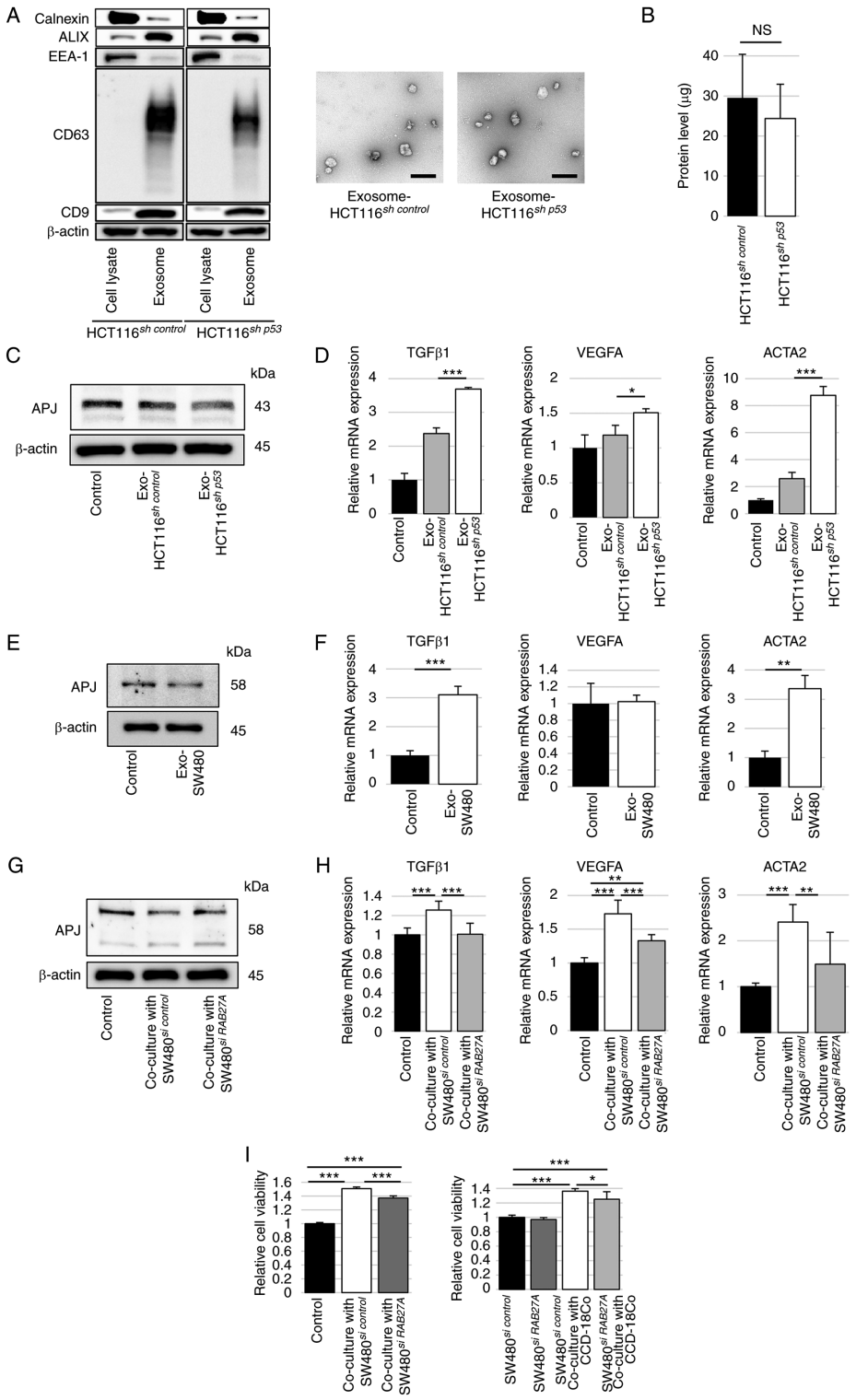

Figure 5. Exosomes derived from TP53-deficient colon cancer cells suppress APJ expression in CCD-18Co cells. (A) Western blot analysis was performed to assess exosomal specific markers ALIX, CD63 and CD9 and exosome-negative proteins calnexin and EEA-1 using cell lysates or isolated pellets from HCT116$^{sh\ control}$ or HCT116$^{sh\ p53}$ cells (left). Representative images of transmission electron microscopy for particles isolated from HCT116$^{sh\ control}$ or HCT116$^{sh\ p53}$ cells culture supernatants (right). Scale bar, 200 nm. (B) Protein levels in pellets isolated from HCT116$^{sh\ control}$ or HCT116$^{sh\ p53}$ cell culture supernatants. (C) Western blot analysis of APJ in CCD-18Co cells treated with HCT116$^{sh\ control}$ or HCT116$^{sh\ p53}$ cell-derived exosomes. The immunoblots were performed three times. (D) RT-qPCR was performed to assess TGFβ1, VEGFA and ACTA2 mRNA expression in CCD-18Co cells treated with HCT116$^{sh\ control}$ or HCT116$^{sh\ p53}$ cell-derived exosomes. (E) Western blot analysis of APJ in CCD-18Co cells treated with SW480 cell-derived exosomes. The immunoblots were performed three times. (F) RT-qPCR was performed to evaluate TGFβ1, VEGFA and ACTA2 mRNA expression in CCD-18Co cells treated with SW480 cell-derived exosomes. (G) Western blot analysis was performed for APJ in CCD-18Co cells co-cultured with SW480 cells with or without siRNA against RAB27A. The immunoblots were performed three times. (H) RT-qPCR was performed to investigate TGFβ1, VEGFA and ACTA2 mRNA expression in CCD-18Co cells co-cultured with SW480 cells with or without RAB27A siRNA. (I) WST assay of CCD-18Co cells co-cultured with SW480 cells with RAB27A siRNA compared with si control (left). WST assay of SW480 cells with or without siRNA against RAB27A and CCD-18Co cells (right). Data are presented as the mean ± SD. A one-way ANOVA with Tukey's post hoc test was performed to analyze the differences among multiple groups. *P<0.05, **P<0.01 and ***P<0.001. APJ, apelin receptor; RT-qPCR, reverse transcription quantitative PCR; ALIX, ALG-2 interacting protein X; EEA-1, early endosome antigen 1; CD63, cluster of differentiation 63; CD9, cluster of differentiation 9; shRNA, short hairpin RNA; NS, not significant; Exo, exosome; siRNA, short interfering RNA.

exosomes (Figs. 5E and S7B). The relative mRNA expression levels of TGFβ1 and ACTA2 were significantly increased in CCD-18Co cells with SW480-derived exosomes, as observed in HCT116$^{sh\ p53}$-derived exosomes (Fig. 5F). Exosome inhibition was evaluated using siRNA against RAB27A, a regulator of exosome secretion. APJ expression in CCD-18Co cells, suppressed by co-culture with SW480 cells, was restored by suppressing RAB27A in SW480 cells (Figs. 5G and S7C). The mRNA expression of TGFβ1, VEGF-A and ACTA2 in CCD-18Co cells, which were increased by being co-cultured with SW480 cells, were significantly decreased by suppressing RAB27A in SW480 cells (Fig. 5H). The WST assay revealed that the viability of CCD-18Co cells, which was increased by co-culturing with SW480 cells, was significantly decreased by the suppression of RAB27A in SW480 cells. Furthermore, the proliferation of SW480 cells, which was increased by co-culture with CCD-18Co cells, was reduced significantly by the suppression of RAB27A in SW480 cells (Fig. 5I).

miR-5703 suppresses APJ expression in fibroblasts. As a mechanism of APJ suppression in fibroblasts, the role of miRNAs in cancer cell-derived exosomes was investigated. The list of miRNAs targeting the APJ gene was created using the miR-DB database and the miRNA profile in HCT116$^{sh\ control}$ and HCT116$^{sh\ p53}$-derived exosomes was analyzed using the registered results of the miRNA microarray analysis (NCBI GEO accession no. GSE120012). A total of 55 miRNAs targeting the APJ gene were detected in HCT116$^{sh\ control}$ and HCT116$^{sh\ p53}$-derived exosomes. Of the 55 miRNAs, 49 were found to be highly expressed in HCT116$^{sh\ p53}$-derived exosomes compared with those of HCT116$^{sh\ control}$. Among them, miR-5703 was identified as the miRNA with the highest expression in HCT116$^{sh\ p53}$-derived exosomes compared with those of HCT116$^{sh\ control}$ (Fig. 6A).

Next, exosomes were collected from HCT116$^{sh\ control}$ and HCT116$^{sh\ p53}$ cell culture supernatants by ultracentrifugation and the expression ratio of miRNAs was validated using RT-qPCR analysis. The relative expression level of miR-5703 was significantly higher in HCT116$^{sh\ p53}$-derived exosomes than in HCT116$^{sh\ control}$-derived exosomes (Fig. 6B). The miRNA mimic was transfected into CCD-18Co cells to investigate the effect of the miRNA on APJ expression in fibroblasts; then, the APJ protein expression of CCD-18Co cells was suppressed and the mRNA expression levels of TGFβ1 and VEGF-A in CCD-18Co cells were significantly increased compared with the control (Figs. 6C and S8A). In addition, the WST assay was performed to investigate the viability of CCD-18Co cells treated with the miRNA mimic, which was significantly higher than that of the control (Fig. 6D). The effects of a specific miR-5703 inhibitor were also explored. Transfection of the miR-5703 inhibitor into CCD-18Co cells after co-culturing with SW480 cells restored the APJ expression in CCD-18Co cells, which was suppressed in the co-cultured SW480 cells (Figs. 6E and S8B). The WST assay revealed that the viability of CCD-18Co cells, which was increased by co-culturing with SW480 cells, was significantly decreased by transfection of the miR-5703 inhibitor into CCD-18Co cells. Finally, the effect of the miR-5703 inhibitor on fibroblast-mediated cancer cell growth was investigated. The miR-5703 inhibitor suppressed the proliferation of SW480 cells co-cultured with CCD-18Co cells (Fig. 6F).

Discussion

The present study revealed that TP53-functional deficient colorectal cancer cells induce the fibroblast-to-myofibroblast transition via suppression of APJ expression in co-existing fibroblasts, and APJ suppression in fibroblasts increases proliferation and migration abilities and accelerates tumor growth. It was also revealed that specific miRNAs encapsulated in cancer cell-derived exosomes play a pivotal role in the mechanism by which TP53-functional deficient cancer cells suppress APJ expression in fibroblasts. In addition, a specific miRNA inhibitor can restore APJ expression in fibroblasts and suppress fibroblast-mediated tumor cell growth.

Previous studies have reported that the APJ system in fibroblasts functioned as a mechanism of suppression of fibroblast-to-myofibroblast transition and related non-neoplastic organ fibrosis such as heart, lung, liver, skin, or kidney; furthermore, one of the mechanisms by which apelin can exert a protective effect against the fibrosis is considered to be the suppression of the TGFβ-Smad pathway (18,19). For instance, activation of the APJ pathway has been reported to exert diverse physiological effects, including anti-fibrotic and anti-remodeling effects, leading to cardiovascular protection (16). The APJ pathway is also closely related to renal fibrosis and improves renal interstitial fibrosis via inhibition of phosphorylated Smad2/3 induced by TGFβ-stimulation (19). There are studies that in pulmonary fibrosis, the apelin-APJ system inhibits the phosphorylation of Smad2/3 and suppresses extracellular matrix production induced by TGF-β (27), and in renal tubular epithelial cells, it inhibits phosphorylated Smad2/3 via activation of PKC-ε (28). It was posited by the authors that the apelin-APJ system could inhibit tumor-promoting CAFs, especially in acquiring myofibroblast-like characteristics. Tumor-promoting CAFs are generally reported to be activated by various factors and show a myofibroblast-like phenotype represented by increased α-SMA expression (7). In addition, it was stated in the Consensus Molecular Subtypes classification that colorectal cancer with strong stromal response type has a poor prognosis (29). To the best of the authors' knowledge, the present study is the first to demonstrate that the APJ system can function as an inhibitory pathway for CAFs, and that suppression of the APJ pathway in fibroblasts by cancer cells promotes tumor progression.

Several studies have focused on the significance of the APJ pathway in cancer cells but not in CAFs. Apelin signaling in cancer cells has been reported to have a tumor-promoting effect via the PI3k/Akt pathway or the activation of Notch3 and STAT3 (22,30). The mRNA and protein levels of apelin and APJ in colorectal cancer are reportedly higher than in control tissues (31). The overexpression of apelin and APJ has also been demonstrated by immunohistochemistry in human colon adenomas and adenocarcinomas (20). The expression levels of apelin and APJ have also been reported to be associated with poor prognosis in malignant tumors of several organs, such as breast cancer (32), cervical cancer (33), ovarian cancer (30) and colorectal cancer (21). These data suggest that both apelin and APJ expression concurrently increase and create an autocrine loop, leading to cancer progression. These findings regarding the apelin-APJ system in cancer cells differ from the suppressed expression of APJ in fibroblasts demonstrated in the present study. As apelin signaling in cancer cells is considered to

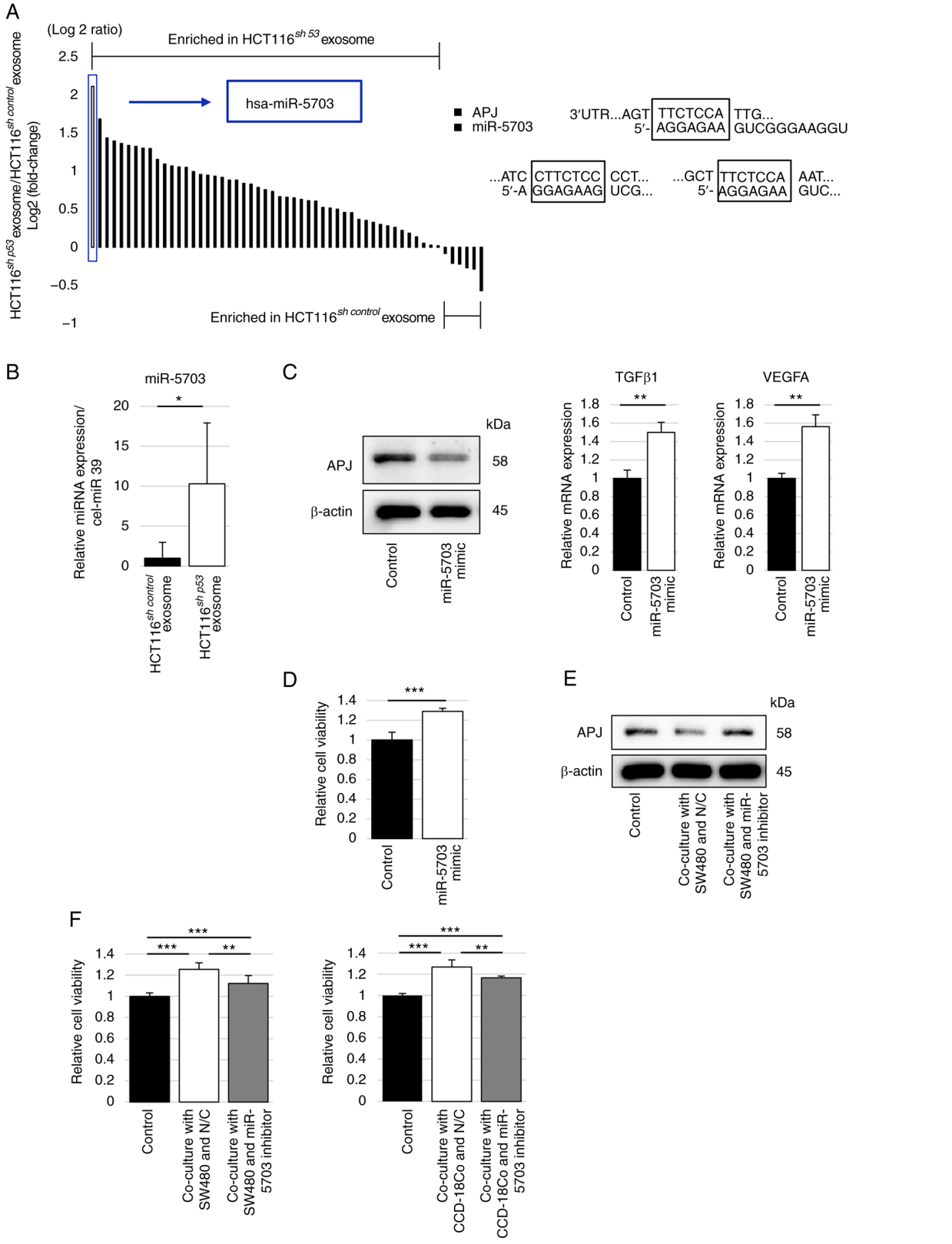

Figure 6. MiR-5703 suppresses APJ expression in CCD-18Co cells. (A) Fold change in the expression profile of identified miRNAs that can suppress APJ gene expression; expression levels in exosomes derived from HCT116$^{sh\ p53}$ cells relative to those from HCT116$^{sh\ control}$ cells. Among them, miR-5703 was identified as the miRNA with the highest expression in exosomes derived from HCT116$^{sh\ p53}$ cells compared with those from HCT116$^{sh\ control}$ cells. (B) RT-qPCR was performed to assess miR-5703 relative expression in exosomes derived from HCT116$^{sh\ p53}$ cells compared with those from HCT116$^{sh\ control}$ cells. (C) Western blot analysis of APJ in CCD-18Co cells with miR-5703 mimic (left). The immunoblots were performed three times. RT-qPCR was performed to evaluate TGFβ1 and VEGFA mRNA expression in CCD-18Co cells with the miR-5703 mimic (right). (D) WST assay of CCD-18Co cells with the miR-5703 mimic compared with control. (E) Western blot analysis of APJ in CCD-18Co cells treated with or without the miR-5703 inhibitor when co-cultured with SW480 cells. The immunoblots were performed three times. (F) WST assay of CCD-18Co cells co-cultured with SW480 cells treated with or without miR-5703 inhibitor (left). WST assay of SW480 cells co-cultured with CCD-18Co cells treated with or without the miR-5703 inhibitor (right). Data are presented as the mean ± SD. A one-way ANOVA with Tukey's post hoc test was performed to analyze the differences among multiple groups. *P<0.05, **P<0.01 and ***P<0.001. shRNA, short hairpin RNA; miR, microRNA; APJ, apelin receptor; RT-qPCR, reverse transcription quantitative PCR; N/C, negative control.

accelerate tumor growth, inhibition of the apelin-APJ system is a possible therapeutic target. Indeed, Hall *et al* (34) demonstrated that inhibition of the apelin-APJ axis using ML221 suppressed tumor growth *in vitro* and in a xenograft model of cholangiocarcinoma cells. However, contrary to the tumor-suppressive effect of ML221 in cancer cells, it was revealed that APJ inhibition in fibroblasts using ML221 induced the modification of myofibroblast-like properties, and the APJ-suppressed fibroblasts showed a tumor-promoting effect. Therefore, it was considered that the systemic administration of an APJ inhibitor may contribute to tumor suppression owing to its antitumor effect on cancer cells. However, the APJ inhibitor can have opposite tumor-promoting effects by affecting the tumor stroma.

Several mechanisms for tumor-promoting CAFs have been reported, including proliferation, activation, trans-differentiation and recruitment (8). Activation of normal tissue fibroblasts is considered one of the origins of CAFs, and diverse types of liquid factors, such as growth factors, cytokines, or chemokines secreted from cancer cells, have been reported to affect normal tissue fibroblasts for the acquisition of a CAF-like phenotype (8). Exosomes are crucial cell-to-cell communication tools in the tumor microenvironment (35). Exosomes derived from donor cells capsulize various gene-expression modulators, such as miRNAs, and can transport them to recipient cells and modulate specific gene expression in recipient cells (36,37). The present study revealed that exosomes derived from cancer cells with p53 deficiency contain higher miRNAs that suppress APJ expression in fibroblasts. Among these, focus was addressed on the expression of miR-5703. Although in a previous study, miR-5703 was reported to be involved in breast cancer and bone metastasis by targeting the Runx2 pathway (38), the present study was the first to identify that miR-5703 could suppress APJ expression in fibroblasts and promote tumor progression. The administration of a miRNA inhibitor restored APJ expression in fibroblasts, which was downregulated in p53-mutant colon cancer cells. Furthermore, a specific inhibitor suppressed fibroblast-mediated cancer cell growth. It was considered that the apelin-APJ system in the cancer stroma and miRNA-mediated APJ suppression in fibroblasts could be novel therapeutic targets.

In the present study, it was revealed that APJ-suppressed fibroblasts increased the proliferation of colon cancer cells and accelerated tumor growth in a xenograft model. However, the details of these mechanisms remain unclear. Furthermore, in the histological analysis of advanced stage tumors, numerous cancer cells harbor p53 mutations, and several different cell types (including fibroblasts) are intermingled. Because the interaction between cancer cells and fibroblasts in advanced stage tumors is difficult to understand and therefore not particularly appropriate considering the focus of the present study, the current analysis was restricted to tissue samples corresponding to early colorectal cancers. Further research is needed to confirm the clinical value of the present findings regarding the miRNA-mediated mechanisms by which normal tissue fibroblasts acquire the CAF-like phenotype and tumor-promoting effects in clinical settings. Developing a delivery system for the inhibitor of specific miRNAs to target the cancer stroma is also required to use the miRNA inhibitor as a therapeutic tool. Despite these limitations, the present study revealed a novel mechanism of fibroblast modification into a CAF-like phenotype. As aforementioned, the fibrotic infiltration in the tumor stroma may be associated with APJ-suppressed fibroblasts. As previously reported, colorectal cancer with strong stromal response type has a poor prognosis (29), and therefore it is conceivable that APJ-suppressed fibroblasts may be associated with colorectal cancer prognosis. Further research on this issue is warranted. p53-functional deficiency in colorectal cancer cells induces fibroblast modification via exosomal miRNAs. Targeting the apelin-APJ system in the cancer stroma may be a novel therapeutic strategy for p53-functional deficient colorectal cancer.

Acknowledgements

Not applicable.

Funding

The present study was supported by JSPS KAKENHI (grant no. JP21K15922) from the Ministry of Education, Culture, Sports, Science and Technology of Japan.

Availability of data and materials

The datasets used and/or analyzed during the current study are available from the corresponding author on reasonable request.

Authors' contributions

HS conceptualized the study, conducted formal analysis and investigation, performed data visualization and wrote the original draft; and contributed equally to data validation and providing methodology. YH conceptualized the study and contributed equally to formal analysis and writing-reviewing and editing the manuscript, and supported supervision. SY conceptualized the study, conducted investigation and contributed equally to writing-reviewing and editing the manuscript. EK, KN, MK, RU, TI and AS contributed equally to conducting investigation and supported writing-reviewing and editing the manuscript. TY, YT, SS and HI contributed equally to conducting investigation and writing-reviewing and editing the manuscript. TT conceptualized and supervised the study, and contributed equally to writing-reviewing and editing the manuscript. HS and YH confirm the authenticity of all the raw data. All authors have read and approved the final manuscript.

Ethics approval and consent to participate

The present study was approved (approval no. 20061) by the Ethics Committee of Osaka University Graduate School of Medicine (Osaka, Japan). Written informed consent was obtained from all patients who provided resected specimens. The study design adhered to the principles of the Declaration of Helsinki (October 2013). The animal experimental procedures were performed per the Osaka University guidelines for animal experiments and were approved (approval no. 30-015-077) by the Animal Care and Use Committee of Osaka University Graduate School of Medicine (Osaka, Japan).

Patient consent for publication

Not applicable.

Competing interests

The authors declare that they have no competing interests.

References

1. Siegel RL, Miller KD, Fuchs HE and Jemal A: Cancer statistics. CA Cancer J Clin 71: 7-33, 2021.
2. Park JW, Seo MJ, Cho KS, Kook MC, Jeong JM, Roh SG, Cho SY, Cheon JH and Kim HK: Smad4 and p53 synergize in suppressing autochthonous intestinal cancer. Cancer Med 11: 1925-1936, 2022.
3. Villalba M, Evans SR, Vidal-Vanaclocha F and Calvo A: Role of TGF-β in metastatic colon cancer: It is finally time for targeted therapy. Cell Tissue Res 370: 29-39, 2017.
4. André T, Shiu KK, Kim TW, Jensen BV, Jensen LH, Punt C, Smith D, Garcia-Carbonero R, Benavides M, Gibbs P, *et al*: Pembrolizumab in microsatellite-instability-high advanced colorectal cancer. N Engl J Med 383: 2207-2218, 2020.
5. Cremolini C, Loupakis F, Antoniotti C, Lupi C, Sensi E, Lonardi S, Mezi S, Tomasello G, Ronzoni M, Zaniboni A, *et al*: FOLFOXIRI plus bevacizumab versus FOLFIRI plus bevacizumab as first-line treatment of patients with metastatic colorectal cancer: updated overall survival and molecular subgroup analyses of the open-label, phase 3 TRIBE study. Lancet Oncol 16: 1306-1315, 2015.
6. Arnold D, Lueza B, Douillard JY, Peeters M, Lenz HJ, Venook A, Heinemann V, Van Cutsem E, Pignon JP, Tabernero J, *et al*: Prognostic and predictive value of primary tumour side in patients with RAS wild-type metastatic colorectal cancer treated with chemotherapy and EGFR-directed antibodies in six randomized trials. Ann Oncol 28: 1713-1729.
7. Togo S, Polanska UM, Horimoto Y and Orimo A: Carcinoma-associated fibroblasts are a promising therapeutic target. Cancers (Basel) 5: 149-169, 2013.
8. Sahai E, Astsaturov I, Cukierman E, DeNardo DG, Egeblad M, Evans RM, Fearon D, Greten FR, Hingorani SR, Hunter T, *et al*: A framework for advancing our understanding of cancer-associated fibroblasts. Nat Rev Cancer 20: 174-186, 2020.
9. Czekay RP, Cheon DJ, Samarakoon R, Kutz SM and Higgins PJ: Cancer-associated fibroblasts: Mechanisms of tumor progression and novel therapeutic targets. Cancers 14: 1231, 2022.
10. Leroy B, Anderson M and Soussi T: TP53 mutations in human cancer: Database reassessment and prospects for the next decade. Hum Mutat 35: 672-688, 2014.
11. Hayashi Y, Tsujii M, Kodama T, Akasaka T, Kondo J, Hikita H, Inoue T, Tsujii Y, Maekawa A, Yoshii S, *et al*: p53 functional deficiency in human colon cancer cells promotes fibroblast-mediated angiogenesis and tumor growth. Carcinogenesis 37: 972-984, 2016.
12. Yoshii S, Hayashi Y, Iijima H, Inoue T, Kimura K, Sakatani A, Nagai K, Fujinaga T, Hiyama S, Kodama T, *et al*: Exosomal microRNAs derived from colon cancer cells promote tumor progression by suppressing fibroblast TP53 expression. Cancer Sci 110: 2396-2407, 2019.
13. Tatemoto K, Hosoya M, Habata Y, Fujii R, Kakegawa T, Zou MX, Kawamata Y, Fukusumi S, Hinuma S, Kitada C, *et al*: Isolation and characterization of a novel endogenous peptide ligand for the human APJ receptor. Biochem Biophys Res Commun 251: 471-476, 1998.
14. Masoumi J, Jafarzadeh A, Khorramdelazad H, Abbasloui M, Abdolalizadeh J and Jamali N: Role of apelin/APJ axis in cancer development and progression. Adv Med Sci 65: 202-213, 2020.
15. Narayanan S, Harris DL, Maitra R and Runyon SP: Regulation of the apelinergic system and its potential in cardiovascular disease: Peptides and small molecules as tools for discovery. J Med Chem 58: 7913-7927, 2015.
16. Nagpal V, Rai R, Place AT, Murphy SB, Verma SK, Ghosh AK and Vaughan DE: MiR-125b is critical for fibroblast-to-myofibroblast transition and cardiac fibrosis. Circulation 133: 291-301, 2016.
17. Kim J: Apelin-APJ signaling: A potential therapeutic target for pulmonary arterial hypertension. Mol Cells 37: 196-201, 2014.
18. Yokoyama Y, Sekiguchi A, Fujiwara C, Uchiyama A, Uehara A, Ogino S, Torii R, Ishikawa O and Motegi SI: Inhibitory regulation of skin fibrosis in systemic sclerosis by apelin/APJ signaling. Arthritis Rheumatol 70: 1661-1672, 2018.
19. Wang LY, Diao ZL, Zhang DL, Zheng JF, Zhang QD, Ding JX and Liu WH: The regulatory peptide apelin: A novel inhibitor of renal interstitial fibrosis. Amino Acids 46: 2693-2704, 2014.
20. Picault FX, Chaves-Almagro C, Projetti F, Prats H, Masri B and Audigier Y: Tumour co-expression of apelin and its receptor is the basis of an autocrine loop involved in the growth of colon adenocarcinomas. Eur J Cancer 50: 663-674, 2014.
21. Zuurbier L, Rahman A, Cordes M, Scheick J, Wong TJ, Rustenburg F, Joseph JC, Dynoodt P, Casey R, Drillenburg P, *et al*: Apelin: A putative novel predictive biomarker for bevacizumab response in colorectal cancer. Oncotarget 8: 42949-42961, 2017.
22. Chen T, Liu N, Xu GM, Liu TJ, Liu Y, Zhou Y, Huo SB and Zhang K: Apelin13/APJ promotes proliferation of colon carcinoma by activating notch3 signaling pathway. Oncotarget 8: 101697-101706, 2017.
23. Livak KJ and Schmittgen TD: Analysis of relative gene expression data using real-time quantitative PCR and the 2(-Delta Delta C(T)) method. Methods 25: 402-408, 2001.
24. Wang P, Liang J, Wang Z, Hou H, Shi L and Zhou Z: The prognostic value of p53 positive in colorectal cancer: A retrospective cohort study. Tumour Biol 39: 1010428317703651, 2017.
25. Trivedi M, Talekar M, Shah P, Ouyang Q and Amiji M: Modification of tumor cell exosome content by transfection with wt-p53 and microRNA-125b expressing plasmid DNA and its effect on macrophage polarization. Oncogenesis 5: e250, 2016.
26. Cooks T, Pateras IS, Jenkins LM, Patel KM, Robles AI, Morris J, Forshew T, Appella E, Gorgoulis VG and Harris CC: Mutant p53 cancers reprogram macrophages to tumor-supporting macrophages via exosomal miR-1246. Nat Commun 9: 771, 2018.
27. Shen J, Feng J, Wu Z, Ou Y, Zhang Q, Nong Q, Wu Q, Li C, Tan X, Ye M, *et al*: Apelin prevents and alleviates crystalline silica-induced pulmonary fibrosis via inhibiting transforming growth factor beta 1-triggered fibroblast activation. Int J Biol Sci 19: 4004-4019, 2023.
28. Wang LY, Diao ZL, Zheng JF, Wu YR, Zhang QD and Liu WH: Apelin attenuates TGF-β1-induced epithelial to mesenchymal transition via activation of PKC-ε in human renal tubular epithelial cells. Peptides 96: 44-52, 2017.
29. Guinney J, Dienstmann R, Wang X, Reynies A, Schlicker A, Soneson C, Marisa L, Roepman P, Nyamundanda G, Angelino P, *et al*: The consensus molecular subtypes of colorectal cancer. Nat Med 21: 1350-1356, 2015.
30. Neelakantan D, Dogra S, Devapatla B, Jaiprasart P, Mukashyaka MC, Janknecht R, Dwivedi SK, Bhattacharya R, Husain S, Ding K and Woo S: Multifunctional APJ pathway promotes ovarian cancer progression and metastasis. Mol Cancer Res 17: 1378-1390, 2019.
31. Podgórska M, Diakowska D, Pietraszek-Gremplewicz K, Nienartowicz M and Nowak D: Evaluation of apelin and apelin receptor level in the primary tumor and serum of colorectal cancer patients. J Clin Med 8: 1513, 2019.
32. Hu D, Cui Z, Peng W, Wang X, Chen Y and Wu X: Apelin is associated with clinicopathological parameters and prognosis in breast cancer patients. Arch Gynecol Obstet 306: 1185-1195, 2022.
33. Yusha C, Lin X, Zheng J, Chen J, Xue H and Zheng X: APLN: A potential novel biomarker for cervical cancer. Sci Prog 104: 368504211011341, 2021.
34. Hall C, Ehrlich L, Venter J, O'Brien A, White T, Zhou T, Dang T, Meng F, Invernizzi P, Bernuzzi F, *et al*: Inhibition of the apelin/apelin receptor axis decreases cholangiocarcinoma growth. Cancer Lett 386: 179-188, 2017.
35. Kosaka N, Yoshioka Y, Fujita Y and Ochiya T: Versatile roles of extracellular vesicles in cancer. J Clin Invest 126: 1163-1172, 2016.
36. Valadi H, Ekström K, Bossios A, Sjöstrand M, Lee JJ and Lötvall JO: Exosome-mediated transfer of mRNAs and microRNAs is a novel mechanism of genetic exchange between cells. Nat Cell Biol 9: 654-659, 2007.
37. Zhang Y, Liu D, Chen X, Li J, Li L, Bian Z, Sun F, Lu J, Yin Y, Cai X, *et al*: Secreted monocytic miR-150 enhances targeted endothelial cell migration. Mol Cell 39: 133-144, 2010.
38. Pranavkrishna S, Sanjeev G, Akshaya RL, Rohini M and Selvamurugan N: A computational approach on studying the regulation of TGF-β1-stimulated Runx2 expression by microRNAs in human breast cancer cells. Comput Biol Med 137: 104823, 2021.